Diffusion-weighted MR imaging in chronic non-bacterial osteitis: Proof-of-concept of the apparent diffusion coefficient as an outcome measure

Jakob M Møller[1,2] ⓘ, **Caroline M Andreasen**[3,4], **Thomas W Buus**[5,6], **Susanne J Pedersen**[7], **Mikkel Østergaard**[2,7], **Henrik S Thomsen**[1,2] ⓘ and **Anne G Jurik**[5,6]

Abstract

Background: The apparent diffusion coefficient (ADC), as determined by whole-body diffusion-weighted MRI, may be useful as an outcome measure for monitoring response to treatment in chronic non-bacterial osteitis.

Purpose: To test and demonstrate the feasibility of ADC-measurement methods for use as outcome measure in chronic non-bacterial osteitis.

Materials and Methods: Using data from a randomized pilot study, feasibility of change-score ADC between baseline and second MRI (ΔADC_{12}) and third MRI (ΔADC_{13}) as outcome measure was assessed in three settings: "whole-lesion," "single-slice per lesion," and "index-lesion per patient". Bone marrow edema lesions were depicted on short tau inversion recovery sequence at baseline and copied to ADC maps at the three time-points. Correlations between the three settings were measured as were analysis of variances. Discriminant validity was assessed as inter- and intra-observer reproducibility and smallest detectable change.

Results: 12 subjects were enrolled, and MRI was performed at baseline and weeks 12 and 36. Pearson correlation was high ($r > 0.86$; $p \leq 0.01$) for ΔADC between single-slice—whole-lesion and whole-lesion—index-lesion and tended to be significant for single-slice—index-lesion settings ($p = 0.06$). For ΔADC_{12} and ΔADC_{13}, Bland–Altman plots showed small differences (0.02, 0.03) and narrow 95% limits-of-agreement (-0.13–0.09, -0.07–0.05 μm^2/s) between whole-lesion and single-slice ROI settings. Inter-observer reproducibility measured by intra-class correlation coefficient was poor-to-fair (range: 0.09–0.31), whereas intra-observer reproducibility was good-to-excellent (range: 0.67–0.90). Smallest detectable changes were between 0.21–0.28 μm^2/s.

Conclusion: ADC change-score as outcome measure was feasible, and the single-slice per lesion ROI setting performed almost equally to whole-lesion setting resulting in reduced assessment time.

[1]Department of Radiology, Herlev-Gentofte Hospital, Herlev, Denmark
[2]Department of Clinical Medicine, University of Copenhagen, Copenhagen, Denmark
[3]Department of Rheumatology, Aarhus University Hospital, Aarhus, Denmark
[4]Department of Medicine, Rheumatology, Vejle Hospital, Vejle, Denmark
[5]Department of Radiology, Aarhus University Hospital, Aarhus, Denmark
[6]Department of Clinical Medicine, Aarhus University Hospital, Aarhus, Denmark
[7]Copenhagen Center for Arthritis Research, Center for Rheumatology and Spine Diseases, Rigshospitalet, Glostrup, Denmark

Corresponding author:
Jakob M. Møller, Department of Radiology, Herlev Hospital, Borgmester Ib Juuls vej 17, DK-2730, Denmark.
Email: jakob.moeller@regionh.dk

Introduction

Chronic non-bacterial osteitis (CNO) is a rare auto-inflammatory disease which is also known as chronic recurrent multifocal osteitis and the synovitis, acne, pustulosis, hyperostosis, and osteitis syndrome. CNO is characterized by relapsing episodes of osteoarticular inflammation. In children/adolescents, the long tubular bones of the lower extremities are the most commonly involved bones, followed by the spine and the clavicles.[1] In adults, the main sites involved are the anterior chest wall followed by the spine and the pelvic bones.[2] Clinical presentations range from mild and limited unifocal disease to severe, chronic inflammation of multiple bones.[3] Extra-skeletal skin and bowel manifestations may occur. Non-steroidal anti-inflammatory drugs are usually used as first-line therapy resulting in control of symptoms in more than 50% of patients. Treatment with the bisphosphonate pamidronate or tumor necrosis factor inhibitors has been suggested as second-line treatment if the response to non-steroidal anti-inflammatory drugs is insufficient. Bisphosphonates inhibit the bone resorption caused by osteoclastic activity and may suppress production of pro-inflammatory cytokines.[4]

Diagnostic imaging in CNO relies on a multi-modality approach where a bone biopsy may be ultimately necessary to exclude malignancy and infection.[5,6] The most characteristic bone lesion in CNO is osteitis. On X-rays, osteitis can be homogeneous or show areas of osteolysis and sclerosis, and hyperostosis is common, especially in adults.[1] X-ray is the first step to identify lesions, and computed tomography may be used for further characterization especially in the anterior chest wall where x-rays demonstrate abnormalities poorly. Since soft tissue and bone marrow edema (BME) is characteristic for active lesions, fat-saturated fluid sensitive MRI sequences such as short tau inversion recovery (STIR) and other T2-weighted fat-saturation sequences are ideal for detection, whereas T1-weighted sequences are necessary for detecting chronic lesions.[1] To diagnose and monitor the multi-focal appearance of CNO, a whole-body MRI approach is often advantageous because clinical assessment may underestimate disease activity compared to imaging.[7]

There are no established imaging outcome measures in CNO, but recently Andreasen et al.[8] have used BME to measure response to treatment. Another potential imaging outcome measure could be the apparent diffusion coefficient (ADC). Diffusion-weighted MRI (DWI) is a method to measure the diffusion of free fluids in the intercellular space. With this method, inflammation can be quantified by calculating the ADC, which has been done in spondyloarthritis, both for diagnosing and for monitoring response to treatment.[9–11] Whole body (WB) DWI in CNO has been studied in small cross-sectional feasibility studies, in which

DWI could visualize BME and soft tissue edema similar to standard sequences[12] and ADC was significantly higher in lesions compared to normal reference tissue.[13] WB DWI is routinely used to evaluate metastatic and hematological diseases,[14] where guidelines for reporting have been developed and validated.[15,16] Similarly, WB DWI in CNO may be used as an alternative or supplement to STIR to measure inflammation and used as an outcome measure.

Therefore, this proof-of-concept study was undertaken to test the feasibility of WB DWI and take a first step in validating three potential ADC change-score (ΔADC) assessment methods.

The objective was to test and demonstrate the feasibility of ΔADC-measurement methods for potential use as outcome measures in CNO.

Material and methods

Study design

This study used data from a randomized clinical trial where CNO patients were randomized to either pamidronate or placebo. Intravenous pamidronate (or sodium chloride) was injected for three consecutive days at baseline and weeks 12 and 24 with a dose of 1 mg per kg bodyweight per day, max 60 mg. Randomization was performed in blocks of four by the hospital pharmacy. Inclusion criteria for the CNO patients were mono- or multi-focal bone inflammation, Jansson clinical score for non-bacterial osteitis in children and adults ≥39,[5] and/or exclusion of infection and malignancy by biopsy and symptom duration above six weeks. Details are described previously.[8] All participants or guardians gave written informed consent before any study-related procedures. The study was approved by the ethics committee for the Central Denmark Region (ref: 48438), the Danish Medicines Agency (ref. EudraCT 2015-002038-36) and registered at ClinicalTrial. gov (NCT 02594878).

Patient-reported outcomes: A visual analogue scale (VAS) was used for pain where no pain = 0 and worst imaginable pain = 100 and for global health where no impact of daily living = 0 and most severe impact = 100.

MRI technique

Whole-body MRI was performed in a 1.5T system (Ingenia, Philips, Best, the Netherlands) acquiring coronal T1-weighted and STIR and axial STIR from the top of the head to the toes, sagittal STIR of the spine and axial DWI of the truncus area (Table 1) at three time-points: baseline, week 12, and week 36. ADC maps were calculated using all three b values (0, 50, 800 s/mm^2) by standard vendor specific software (Intellispace ver. 9, Philips, Best, the Netherlands).

Table 1. Technical parameters for the MRI sequences used.

Sequence plane	TR (ms)	TE (ms)	TI (ms)	b (s/mm^2)	FOV (mm)	Matrix	ST (mm)	NSA	Gap (mm)	Stations	Time[a] (min: sec)
STIR-SAG	2696	70	165	-	349x180	306x200	4	2	0.4	2	4:24
STIR-AX	8856	60	160	-	550x300	344x160	6	1	1	7	0:18
STIR-COR	8900–9600	60	160	-	549x300	274x188	6	1	1	7	0:18
T1w-COR	307	46	-	-	550x300	287x216	3.4	1	-	7	0:15
DWI-AX	1600	64	180	0; 50; 800	500x275	144x139	6	2	1	3	2:21[b]

[a]Time per station.

[b]Respiratory triggered sequence. Real time approximately 5 min.

AX, axial; COR, coronal; DWI, diffusion weighted imaging with background suppression; FOV, field of view; NSA, number of samplings; T1w, T1-weighted gradient echo; SAG, sagittal; ST, slice thickness; STIR, short tau inversion recovery; TE, echo time; TI, inversion time; TR, repetition time.

Anonymization

All examinations from baseline were anonymized and analyzed using random numbers. The follow-up examinations at 12 and 36 weeks were anonymized with the same random number as baseline with an extension number of 2 and 3, respectively.

Image analysis

Images from all three time-points were available for simultaneous assessment and read in known order. By conventional MRI, BME was assessed as previously described.[8] In short, anterior chest wall inflammation was assessed corresponding to the sternoclavicular, manubriosternal, and sternocostal joints on the STIR sequences and graded according to the subchondral extent of osseous BME; grade 1: ≤1 cm, grade 2: 1–3 cm, and grade 3: >3 cm with an additional score value of 1 for intensity comparable with cerebrospinal fluid; the total max score value was 31. Spinal inflammation was assessed using a modification of the scoring method developed by Madsen et al.[17] encompassing all 23 discovertebral units and graded as follows: grade 1: BME extent <25%, grade 2: 25%–50%, and grade 3 >50% of vertebral endplate area with an additional score of 1 for the presence of BME at apophyseal and costovertebral joints; the total max score value was 81.

Bone lesions were detected on the STIR sequences at the baseline examination or when occurring later on at week 12 or week 36. A freehand region-of-interest (ROI) was drawn to encircle the lesion, and it was copied and applied at the ADC maps at all three time-points. In this area, the mean ADCs were measured. An ADC measurement of a reference ROI of nearby normal bone marrow as judged by the assessor was performed for each lesion. The assessment was performed in three settings: A whole-lesion (WL) approach where all slices in the lesions were measured, a single slice (SS) approach where one slice per lesion was measured, and an index lesion (IL) approach where the most dominant lesion as judged by the assessor was measured. All examinations were read twice with a six weeks interval by the same assessor with > 10 years of experience in muscle skeletal MRI including ADC to measure intra-observer reproducibility, and all examinations were read by another assessor with 3 years of oncologic DWI experience to measure the inter-observer reproducibility.

Statistics

For each baseline lesion, a ratio of ADC to normal bone marrow was calculated. Outcome measures were calculated as the ADC change-scores from week 0 to 12 (ΔADC_{12}) and from week 0 to 36 (ΔADC_{13}). Correlation between the three settings at each time-point was tested using Pearson's r correlation test and using a single measure two-way mixed intra-class correlation coefficient (ICC). Correlation between ΔADC and BME change-score (ΔBME) was tested using Spearman's ρ. ANOVA was used to test ΔADC between the three ROI-settings at each time-point. ΔADC was calculated both for all lesions and separately for anterior chest wall lesions.

Intra- and inter-observer reproducibility were measured using ICC. ICC was interpreted as 0.00–0.20: poor, 0.21–0.40: fair, 0.41–0.60: moderate, 0.61–0.80: good, and 0.81–1.00: excellent.[18] Smallest detectable change was calculated between first and second MRI and first and last MRI as $1.96 \times (SD_{dif})/\sqrt{2}$, where SD_{dif} was the standard deviation of the differences between two scorings performed by the first assessor.[19] Absolute measurement error was further assessed by Bland–Altman plots at each time-point. A probability (p) value of less than 0.05 was considered statistically significant. Statistical analysis was performed using SPSS (ver. 22.0, IBM, Armonk, NY, USA)

Results

Subjects

Fifty-six patients were pre-screened and 24 of them were assessed for eligibility. A total of 13 adult patients and one child provided informed consent and were included; all were followed at the departments of Rheumatology and Pediatric and Adolescent Medicine, Aarhus University Hospital, Denmark. Due to methodological considerations, the child was excluded, as was one adult in the pamidronate group, who did not complete the study (lacks week 36 examinations).

Of the 12 enrolled patients, two in the pamidronate and one in the placebo group did not have DWI MRI performed at baseline and one patient in the placebo group did not have DWI MRI performed at week 36. Despite the randomization procedure, there were differences at baseline regarding age, VAS pain, and VAS global in addition to distribution and activity of CNO lesions (Table 2).

Table 2. Baseline characteristics of patients randomized to pamidronate and placebo.

	Pamidronate ($n = 6$)	Placebo ($n = 6$)
Age (years; median; IQR)	26 (22–35)	53 (26–57)
Sex (female), n	4	5
Symptom duration (year; median (IQR))	14 (11–16)	11 (5–17)
Concomitant NSAIDs	6	3
Concomitant DMARDs	1	1
Concomitant TNF inhibitor	0	1
Concomitant opioids	3	3
VAS pain (median; IQR)	27 (24–54)	49 (23–70)
VAS global (median; IQR)	28 (13–51)	61 (23–71)
HLA B27 positive	1	0
ACW STIR BME score (median; IQR)	5 [4–7]	2[1–4]
ACW ADC (lesions median; IQR)	1[1–1]	1[0.75–2]
Spine STIR BME score (median; IQR)	27	12 [6–15]
Spine ADC (lesions median; IQR)	10	3[1.75–5.5]

ACW, anterior chest wall; ADC, apparent diffusion coefficient; BME, bone marrow edema; DMARDs, disease-modifying-anti-rheumatic-drugs; HLA B27, human leucocyte antigen B27; IQR, inter quartile range; NSAIDs, non-steroid-anti-inflammatory-drugs; STIR, short tau inversion recovery; TNF, tumor-necrosis-factor; VAS, visual analogue scale.

Patient reported outcomes

VAS pain was decreased by 54% in the pamidronate group and increased 4% in the placebo group at week 36, but the changes were not statistically significant ($p = 0.11$). Similarly, VAS global decreased 73% in the pamidronate group and 17% in the placebo group ($p = 0.08$).

Conventional MRI

All patients had active anterior chest wall lesions at baseline, as assessed by STIR images. There was a significant decrease in anterior chest wall activity score from baseline to week 36 in the pamidronate group (5 (inter quartile range (IQR): 4–7) to 2.5 (IQR: 2–3) ($p=0.04$)). In contrast, no change was observed in the placebo group, in which the activity score was 2 (IQR: 1–4) at baseline and 2.5 (IQR: 1–7) at week 36. Two new anterior chest wall lesions were observed in the pamidronate group (Figure 1) and three in the placebo group at week 12. Only one patient in the pamidronate group had spinal lesions. In this patient, the spine activity score decreased from 27 to 20, whereas in the placebo group the median activity score remained unchanged 12 (IQR: 6–15) in the five patients with spinal lesions. In the spine, two new lesions were observed at week 12 and seven at week 36 in the placebo group, versus none in the pamidronate group.

Apparent Diffusion Coefficient

The median lesion to reference bone marrow ratio ADC was 2.08 (IQR:1.67–2.97) for WL and 1.83 (IQR:1.47–2.73) and 1.69 (IQR:1.29–2.50) for SS and IL, respectively. In anterior chest wall, there was a statistically significant negative correlation of ΔBME with ΔADC_{12} for the WL setting ($\rho = -0.76$, $p = 0.02$), but no other significant correlations of ΔBME with ΔADC were revealed.

The mean ΔADCs for the WL, SS, and IL settings were highly correlated at both time-points except ΔADC_{13} for the SS and IL settings (Figure 2), which only tended to be correlated (Table 3). ANOVA did not reveal any significant differences between the three settings for ΔADC_{12} ($p = 0.80$) and ΔADC_{13} ($p = 0.87$). In Bland–Altman plots (Figure 3), the smallest differences (0.02 μm^2) and 95% limits of agreements (-0.13–0.09 μm^2) were found in the WL-SS settings for both ADC_{12} and ADC_{13}.

Intra-observer reproducibility ranged from good (ICC 0.67 (95%CI 0.06–0.91)) to excellent (ICC 0.90 (95%CI 0.54–0.98)), but inter-observer reproducibility was poor (ICC 0.09 (95%CI(-0.75–0.66))) to fair (ICC 0.31 (95%CI: (-0.50–0.84))) (Table 4). Smallest detectable changes are given in Table 4.

No significant ΔADC between the pamidronate and placebo group was revealed.
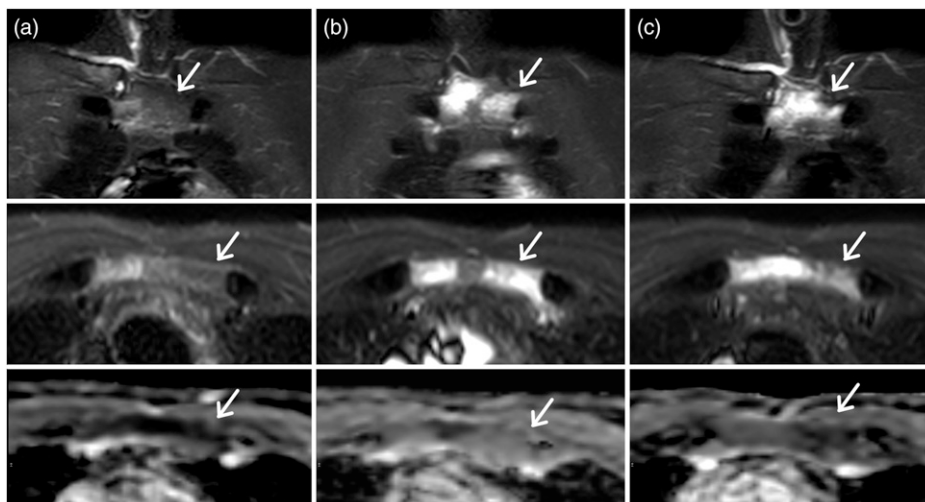
Figure 1. A 61-year-old male with chronic non-bacterial osteitis. MRI images before (a), after 12 weeks (b), and 36 weeks (c) of pamidronate therapy. Coronal STIR images (upper row), axial STIR images (middle row), and axial apparent diffusion coefficient (ADC) maps (lower row) are presented. Compared to baseline (a), an additional lesion in left manubrium (arrow) at week 12 (b) and 36 (c) is visualized.
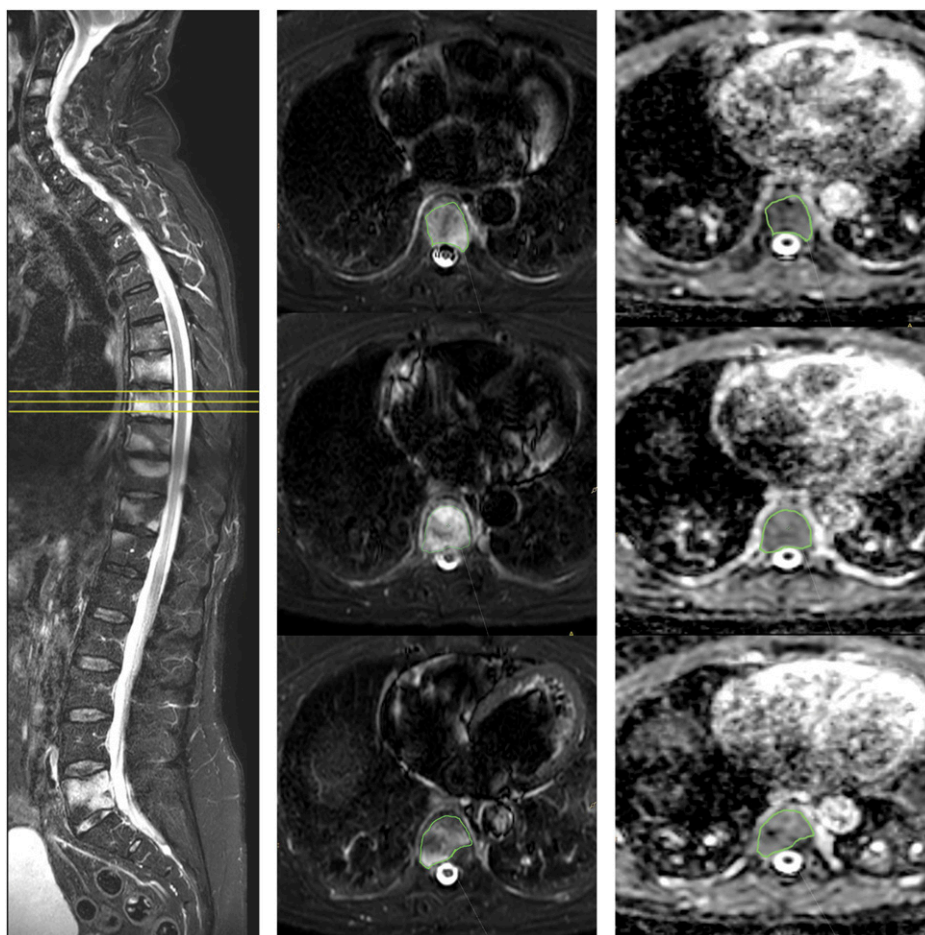

Figure 2. Sagittal short tau inversion recovery (STIR) of the spine showing several vertebrae with bone marrow edema (BME). Three axial STIR with corresponding apparent diffusion coefficient (ADC) slices of the eighth thoracic vertebral body covering the BME lesion. The whole lesion ADC measurement (1.28 $\mu mm^2/s$) is highly correlated to the single slice (middle slice) ADC measurement (1.37 $\mu mm^2/s$).

Discussion

In this study, we found the single-slice ROI setting very similar to the whole-lesion ROI setting which may reduce assessment time. Assessing whole lesion ADC maps by manually drawing ROIs can be a time-consuming procedure.

Table 3. Correlations and differences of mean ADC change-scores from week 0 to 12 (ΔADC_{12}) and from week 0 to 36 (ΔADC_{13}) for the three ROI settings.

	Mean ΔADC SS	Mean ΔADC IL
ΔADC$_{12}$ n = 9		
Mean ΔADC WL		
Pearson's r	0.95; p < 0.01	0.91; p < 0.01
ICC (95%CI)	0.95 (0.80–0.99)	0.88 (0.55–0.97)
Difference (SD)	-0.02 (0.06)	-0.06 (0.11)
Mean ΔADC SS		
Pearson's r		0.89; p < 0.01
ICC (95%CI)		0.85 (0.47–0.96)
Difference (SD)		-0.04 (0.12)
ΔADC$_{13}$ n = 8		
Mean ΔADC WL		
Pearson's r	0.86; p < 0.01	0.95; p < 0.01
ICC (95%CI)	0.82 (0.34–0.96)	0.93 (0.65–0.98)
Difference (SD)	-0.01 (0.03)	-0.04 (0.08)
Mean ΔADC SS		
Pearson's r		0.69; p=0.06
ICC (95%CI)		0.69 (0.05–0.93)
Difference (SD)		-0.03 (0.10)

ΔADC, apparent diffusion coefficient change-score; ΔADC$_{12}$, difference in score between baseline and week 12; ΔADC$_{13}$, difference in score between baseline and week 36; ICC, intra-class correlation coefficient; IL, index lesion; ROI, region of interest; SD, standard deviation; SS, single slice; WL, whole lesion; 95%CI, 95% confidence interval.

ROI must be carefully drawn on every slice of each lesion and for all lesions in each examination, but fortunately, the ADC measure is independent of ROI geometry.[23] In the present study, the use of less time-consuming ROI approaches in the quick SS-setting highly correlated with the much more time-consuming WL-setting. Further, the absolute differences in ΔADC_{12} and ADC$_{13}$ between WL- and SS-setting and the corresponding 95% limits-of-agreement were small.

ADC seems not usable directly as a response measure because it is influenced by age, sex, and anatomical location.[18,19] Thus, in healthy individuals, the ADC of lumbar vertebrae differs according to anatomical location, and spinal ADC has been found dependent on age in females.[18] Therefore, the ΔADC was used in the present study to compensate for baseline variances. ADC change-scores have not been used in other axSpA studies, but change-scores of BME are widely used as outcome measures in studies of spondyloarthritis to compensate for baseline variances.[20–23]

ADC findings similar to ours have been published in other diseases where observer-decided single slice ROI ADC measurements were compared to whole lesion ADC in the soft tissue lesions,[24] parotid glands,[25] and liver.[26] In these studies, the ADC measurements were similar,[24–27] the inter-observer agreement was excellent, and the assessment time was significantly less than by the whole lesion approach.[24,26] A reason for the high correlation of WL and SS in CNO could be that inflamed BME lesions were homogenous and therefore no or little variation in inflammation inside the lesion was present. However, if CNO lesions are homogenously inflamed, an index lesion could be representative for all lesions when monitoring response
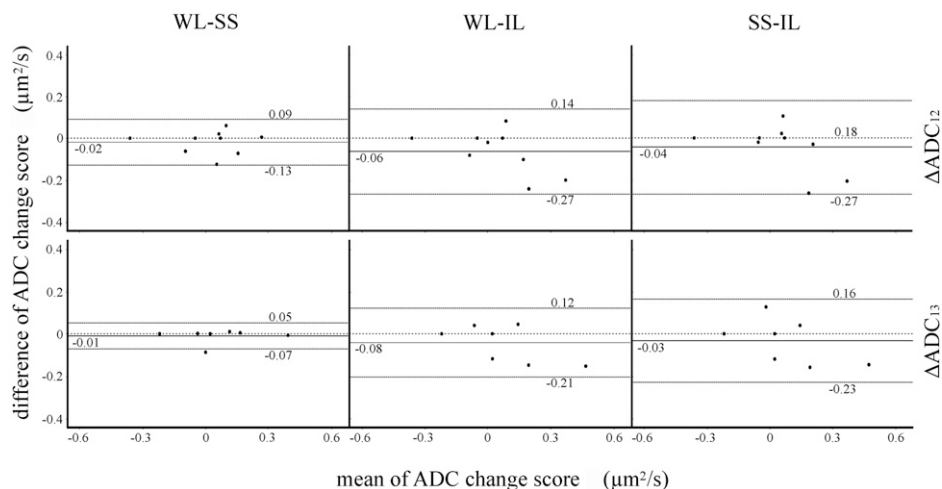

Figure 3. Bland–Altman plots of apparent diffusion coefficient (ADC) change-scores for the three ROI settings. Mean difference (black line) and limits-of-agreement (dotted lines) calculated as 1.96 x standard deviation of the differences provided. ΔADC$_{12}$, ADC change-score between baseline and week 12; ΔADC$_{13}$, ADC change-score between baseline and week 36; IL, index lesion; SS, single slice; WL, whole-lesion.

Table 4. Reliability of ADC change-scores from week 0 to 12 (ΔADC_{12}) and from week 0 to 36 (ΔADC_{13}), intra-class correlation coefficients with 95% confidence interval, and the smallest detectable change (SDC) by the three methods.

	WL	SS	IL
Intra-reader variation ΔADC_{12}	0.75 (0.22–0.94)	0.67 (0.06–0.91)	0.74 (0.14–0.94)
Inter-reader variation ΔADC_{12}	0.13 (−0.59–0.73)	0.16 (−0.56–0.75)	0.19 (−0.54–0.76)
Intra-reader variation ΔADC_{13}	0.84 (0.41–0.97)	0.73 (0.13–0.94)	0.90 (0.54–0.98)
Inter-reader variation ΔADC_{13}	0.25 (−0.60–0.81)	0.09 (−0.75–0.66)	0.31 (−0.50–0.84)
SDC ΔADC_{12}	0.21	0.23	0.25
SDC ΔADC_{13}	0.25	0.28	0.24

to treatment. In the present study, the ΔADC values from the WL- and IL-settings were highly correlated for all change-scores and modestly for the SS- and IL-settings, suggesting that the IL-setting could be used to reflect treatment response. The differences and 95% limits-of-agreement between the WL- and IL-settings were larger than the WL-SS setting, but the assessment time can potentially be reduced even more, but needs to be proved in future studies. A similar target lesion approach was used for monitoring treatment response in Hodgkin lymphoma where a number of target lesions were designated as outcome measures.[28,29]

Discrimination validity reflects that treatment-induced variation of the outcome measure over time is reproducible. Due to the few subjects in this study, it was not possible to measure a treatment-induced variation. However, the smallest detectable changes were determined and were almost similar for both ΔADC outcomes in all three ROI settings.

The lesion to reference bone marrow ratio ADC in the present study was similar to the ratio presented by Leclair et al.[13] where elevated ADC values were measured in inflammatory lesions. Together with the significant correlation of ΔADC with ΔBME in the anterior chest wall, elements of construct validity have been assessed. The depicted lesions on ADC maps reflect true inflammatory lesions.

WB MRI including DWI is today routinely used in oncoradiology for detecting and monitoring diseases. Similar scanning protocols can be used in CNO examinations, both at 1.5T and 3T systems. With the use of 5–7 mm slice-thickness in 3–4 stations, the axial DWI sequence will cover the relevant anatomy. The DWI sequence needs at least two b-values, a low of 50–100 s/mm2 and a high of 800–1000 s/mm2, to calculate the ADC map.[30] The high intra-reader agreement suggests that the lesions were depicted objectively by the first assessor. The only poor–fair inter-reader agreement was probably a result of poor communication and training of the second reader, where sclerotic pattern of the affected bones may have resulted in different delineation performed by the two readers resulting in divergent ADC measurements. Due to the few patients in the study, their lesions might have been recognizable if used during a formalized training where both readers analyzed several cases together and thus potentially introducing observer bias.

This study presents a proof-of-concept which implies several limitations. First, the small number of participants lowered the credibility of the results. Second, the spatial resolution of DWI was three times lower than that of STIR, potentially compromising the interpretation of the ADC maps. Further, the single center setup where all subjects were imaged in the same MRI system by the same radiographer reduced the generalizability. Finally, the only fair inter-observer reproducibility suggested a sub-optimal lesion detection procedure.

In conclusion, a proof-of-concept in validation of ADC change-score was performed, and the single-slice per lesion ROI setting performed almost equally to whole-lesion setting resulting in reduced assessment time, but further validation studies are needed.

Authors Contributions

Andreasen and Jurik planned and initiated the trial.
Andreasen managed all patients. Jurik sat up MRI protocol and had responsibility for obtaining the MRI scans.
Møller and Buus evaluated the whole body MRI.
Østergaard, Pedersen, and Thomsen gave substantial input to assessment and statistical analyses.
Møller performed statistical analyses and drafted the manuscript.
All authors critically revised the manuscript.

Declaration of conflicting interests

The author(s) declared no potential conflicts of interest with respect to the research, authorship, and/or publication of this article.

ORCID iDs

Jakob Møllenbach Møller, ⓘ https://orcid.org/0000-0001-6576-6494

Henrik Segelcke Thomsen, ⓘ https://orcid.org/0000-0002-2409-9725

References

1. Jurik AG, Klicman RF, Simoni P, et al. The value of imaging. Semin Musculoskelet Radiol 2018; 22: 207–24.
2. Leone A, Cassar-Pullicino VN, Casale R, et al. The SAPHO syndrome revisited with an emphasis on spinal manifestations. Skeletal Radiol 2015; 44: 9–24.
3. Miettunen P. Chronic non-bacterial osteitis/chronic recurrent multifocal osteomyelitis. InTech 2012; 89–118.
4. Andreasen CM, Jurik AG, Glerup MB, et al. Response to early-onset pamidronate treatment in chronic nonbacterial osteomyelitis: A retrospective single-center study. J Rrheumatol 2019; 46: 1515–23.
5. Jansson AF, Müller TH, Gliera L, et al. Clinical score for nonbacterial osteitis in children and adults. Arthritis Rheum 2009; 60: 1152–1159.
6. Benhamou CL, Chamot AM and Kahn MF. Synovitis-acne-pustulosis hyperostosis-osteomyelitis syndrome (SAPHO). A new syndrome among the spondyloarthropathies?. Clin Exp Rheumatol 1988; 6: 109–112.
7. Voit AM, Arnoldi AP, Douis H, et al. Whole-body Magnetic Resonance Imaging in Chronic Recurrent Multifocal Osteomyelitis: Clinical Longterm Assessment May Underestimate Activity. J Rheumatol 2015; 42: 1455–1462.
8. Andreasen CM, Jurik AG, Deleuran BW, et al. Pamidronate in chronic non-bacterial osteomyelitis: a randomized, double-blinded, placebo-controlled pilot trial. Scand J Rheumatol 2020; 49: 312–322.
9. Bozgeyik Z, Ozgocmen S and Kocakoc E. Role of diffusion-weighted MRI in the detection of early active sacroiliitis. Am J Roentgenology 2008; 191: 980–986.
10. Gezmis E, Donmez FY and Agildere M. Diagnosis of early sacroiliitis in seronegative spondyloarthropathies by DWI and correlation of clinical and laboratory findings with ADC values. Eur J Radiol 2013; 82: 2316–2321.
11. Gaspersic N, Sersa I, Jevtic V, et al. Monitoring ankylosing spondylitis therapy by dynamic contrast-enhanced and diffusion-weighted magnetic resonance imaging. Skeletal Radiol 2008; 37: 123–131.
12. Neubauer H, Evangelista L, Morbach H, et al. Diffusion-weighted MRI of bone marrow oedema, soft tissue oedema and synovitis in paediatric patients: feasibility and initial experience. Pediatr Rheumatol 2012; 10: 20.
13. Leclair N, Thörmer G, Sorge I, et al. Whole-Body Diffusion-Weighted Imaging in Chronic Recurrent Multifocal Osteomyelitis in Children. PloS one 2016; 11: e0147523.
14. Padhani AR, Koh D-M and Collins DJ. Whole-body diffusion-weighted mr imaging in cancer: current status and research directions. Radiology 2011; 261: 700–718.
15. Messiou C, Hillengass J, Delorme S, et al. Guidelines for acquisition, interpretation, and reporting of whole-body mri in myeloma: myeloma response assessment and diagnosis system (MY-RADS). Radiology 2019; 291: 5–13.
16. Padhani AR, Lecouvet FE, Tunariu N, et al. METastasis reporting and data system for prostate cancer: practical guidelines for acquisition, interpretation, and reporting of whole-body magnetic resonance imaging-based evaluations of multiorgan involvement in advanced prostate cancer. Eur Urol 2017; 71: 81–92.
17. Madsen KB and Jurik AG. MRI grading method for active and chronic spinal changes in spondyloarthritis. Clinical radiology 2010; 65: 6–14.
18. Lambregts DMJ, Beets GL, Maas M, et al. Tumour ADC measurements in rectal cancer: effect of ROI methods on ADC values and interobserver variability. Eur Radiol 2011; 21: 2567–2574.
19. Bruynesteyn K, Boers M, Kostense P, et al. Deciding on progression of joint damage in paired films of individual patients: smallest detectable difference or change. Ann Rheum Dis 2005; 64: 179–182.
20. Braun J, Baraliakos X, Hermann K-G, et al. Effect of certolizumab pegol over 96 weeks of treatment on inflammation of the spine and sacroiliac joints, as measured by MRI, and the association between clinical and MRI outcomes in patients with axial spondyloarthritis. RMD open 2017; 3: e000430.
21. Deodhar A, van der Heijde D, Gensler LS, et al. Ixekizumab for patients with non-radiographic axial spondyloarthritis (COAST-X): a randomised, placebo-controlled trial. Lancet (London, England) 2020; 395: 53–64.
22. Maksymowych WP, Dougados M, van der Heijde D, et al. Clinical and MRI responses to etanercept in early non-radiographic axial spondyloarthritis: 48-week results from the EMBARK study. Ann Rheum Dis 2016; 75: 1328–1335.
23. Sieper J, van der Heijde D, Dougados M, et al. Efficacy and safety of adalimumab in patients with non-radiographic axial spondyloarthritis: results of a randomised placebo-controlled trial (ABILITY-1). Ann Rheum Dis 2013; 72: 815–822.
24. Ahlawat S, Khandheria P, Del Grande F, et al. Interobserver variability of selective region-of-interest measurement protocols for quantitative diffusion weighted imaging in soft tissue masses: comparison with whole tumor volume measurements. J Magn Reson Imaging 2016; 43: 446–454.
25. Xu X, Su G, Hu H, et al. Effects of regions of interest methods on apparent coefficient measurement of the parotid gland in early Sjögren's syndrome at 3T MRI. Acta Radiologica 2017; 58: 27–33.
26. Filipe JP, Curvo-Semedo L, Casalta-Lopes J, et al. Diffusion-weighted imaging of the liver: usefulness of ADC values in the differential diagnosis of focal lesions and effect of ROI

methods on ADC measurements. Magn Reson Mater Phys Biol Med 2013; 26: 303–312.

27. Chung HY, Xu X, Lau VW, et al. Comparing diffusion weighted imaging with clinical and blood parameters, and with short tau inversion recovery sequence in detecting spinal and sacroiliac joint inflammation in axial spondyloarthritis. Clin Exp Rheumatol 2017; 35: 262–269.

28. Albano D, Patti C, Matranga D, et al. Whole-body diffusion-weighted MR and FDG-PET/CT in Hodgkin Lymphoma: Predictive role before treatment and early assessment after two courses of ABVD. Eur J Radiol 2018; 103: 90–98.

29. Cheson BD, Fisher RI, Barrington SF, et al. Recommendations for initial evaluation, staging, and response assessment of hodgkin and non-hodgkin lymphoma: the lugano classification. J Clin Oncol 2014; 32: 3059–3067.

30. Pasoglou V, Michoux N, Larbi A, et al. Whole body MRI and oncology: recent major advances. Br J Radiol 2018; 91: 20170664.